Heavy isotope ^{6}He: Properties of bulk system and of clusters

D. E. Galli and L. Reatto
Istituto Nazionale di Fisica della Materia, Dipartimento di Fisica, Universitá di Milano, Via Celoria 16, 20133 Milano, Italy
(Received 21 December 2000; published 11 May 2001)

We have theoretically revisited the heavy isotope of He, ^{6}He. It was considered many years ago as a possible superfluid system, but its short lifetime makes any experiment rather difficult and theoretical predictions are not very favorable. We have applied the shadow wave-function technique to the study of bulk ^{6}He and we have also studied clusters of ^{6}He. We confirm that the ground state is solid but the energy difference between the two phases is rather small and the solid order is also inhibited in clusters of many hundreds of particles. From a study of the off-diagonal one-body density matrix we find that Bose-Einstein condensation is present in these clusters. Thus clusters of ^{6}He offer the unique opportunity to study the evolution from a superfluid to a solid driven by size effect and the properties of a highly defected quantum solid.

DOI: 10.1103/PhysRevB.63.214515 PACS number(s): 67.80.−s

I. INTRODUCTION

Superfluidity is one of the phenomena of purely quantum-mechanical origin that can arise in a system of interacting indistinguishable particles. This explains the search for other superfluids in addition to the He liquids. Bose-Einstein condensation (BEC) has been achieved with alkali atoms and atomic hydrogen and in the case of alkali atoms evidence for superfluidity has been obtained.[1] With molecular hydrogen BEC is prevented by solidification and ways to contrast solidification have been considered theoretically.[2] A cluster or the free surface of H_2 is not efficient enough to cause a fluid state and only for a microscopically decorated adsorption surface the inhibition of the solid phase appears to be strong enough to leave a kind of modulated superfluid state. No experimental study has been performed yet on such a system.

Another possible superfluid system was considered many years ago: the heavy isotope of He, ^{6}He.[3] Its short lifetime ($\tau_{1/2}=0.82$ sec) makes any experiment very difficult and theoretical predictions are not very favorable. On the basis of quantum corresponding state arguments the ground state of bulk ^{6}He was predicted to be solid, not liquid.[4] In a ^{6}He-^{4}He mixture the estimated transition for the ^{6}He component was so low that phase separation prevents any superfluid behavior.

We have revised the ^{6}He system. In the first place the earlier results[4,5] were based on rather primitive variational theories. In particular those theories gave a better representation of the solid phase than of the fluid one and this might have altered the evaluation of the relative stability of the two phases. Presently the variational theory has progressed to such an extent that both phases are represented very accurately[6] in the case of ^{4}He. In addition local solid order can be described without difficulty in situations like liquid-solid coexistence[7] or in a doped cluster where the solidlike order around the impurity gives way to a fluid state far from the impurity.[8] We confirm on the basis of an advanced variational theory that the ground state is solid but the energy difference between the two phases is rather small. In clusters we find that the solid order is inhibited also in the case of clusters of many hundreds of particles. A large cluster of ^{6}He will offer the unique opportunity to study the evolution from a superfluid to a solid driven by size effect and the possibility of the existence of a supersolid state. We employ here the variational theory based on shadow wave function (SWF). As we comment in the following, this theory is very useful in situations in which a quasicrystalline order sets in.

The contents of the paper are as follows. In Sec. II the variational method used to study bulk and cluster properties of ^{6}He is reviewed. In Sec. III the results are presented for bulk ^{6}He, for one ^{6}He impurity in liquid ^{4}He, and for ^{6}He clusters, whereas in Sec. IV the technique described is used to analyze the off-diagonal long-range order in ^{6}He clusters and the relative results.

II. THE SHADOW WAVE-FUNCTION TECHNIQUE

A. Bulk ground state

The shadow wave-function theory is a powerful variational Monte Carlo method; it consists of using an integral functional form for the trial wave function in order to take into account in an implicit way many-body correlations between particles with the technique of subsidiary variables. In this way one implicitly is introducing many-body correlations and is not limited to two- and three-body correlations as in the case of the standard variational treatments. For a bulk system composed of N ^{6}He atoms we write the shadow wave-function representation of the ground state in the form

$$\Psi_0(R)=\int dS \;\; F(R,S), \tag{1}$$

where $R=\{\vec{r}_1,\ldots,\vec{r}_N\}$ are the coordinates of the particles, and $S=\{\vec{s}_1,\ldots,\vec{s}_N\}$ is a set of auxiliary (shadow) variables that are integrated over the whole space. Interparticle correlations between ^{6}He atoms are contained in

$$F(R,S)=\phi_p(R)\times\prod_{i=1}^{N} f_{ps}(|\vec{r}_i-\vec{s}_i|)\times\phi_s(S). \tag{2}$$

$\phi_p(R)$ and $\phi_s(S)$ are Jastrow factors: $\phi_p(R)=\Pi_{i<j=1}^{N} f_p(|\vec{r}_i-\vec{r}_j|)$ and $\phi_s(S)=\Pi_{i<j=1}^{N} f_s(|\vec{s}_i-\vec{s}_j|)$. We

have used simple parametrized forms for the correlating factors $f_p(r)=\exp[-1/2(b/r)^5]$, and f_s contains a rescaled form of the Aziz potential,[9] which is also used to model the interaction between ^{6}He atoms $f_s(s)=\exp[-\delta v_{AZ}(\alpha s)]$. For the shadow-particle correlations a Gaussian has been used, $f_{ps}(|\vec{r}_i-\vec{s}_i|)=\exp[-C(|\vec{r}_i-\vec{s}_i|)^2]$. This wave function contains four variational parameters b, δ, α, and C, which are determinated by minimization of the expectation value of the Hamiltonian. The computation is standard and details can be found elsewhere.[6] Let us just notice that the essential trick in this Monte Carlo technique is that the integration over the shadow variable is performed stochastically together with the Monte Carlo integration over real variables, so that one has to integrate over $3\times d\times N$ variables, where N is the number of particles in the system and d is the dimensionality. Shadow wave function has been extensively applied to the ^{4}He system in many different physical situations giving superior results[6] not only for the ground state but also for excited states. Probably the most important achievement of this variational technique is that shadow wave functions are able to describe with the same functional form the liquid and solid phases: when one increases the density of the system the correlations between shadow variables become so strong that they drive the system to the solid phase and no *a priori* equilibrium positions have to be introduced.

With the same functional form of SWF it is possible to also represent a ^{4}He system with a finite concentration of ^{6}He impurity atoms. This is completely similar to the calculations we have already done to obtain ground- and excited-state properties of a ^{3}He impurity in liquid bulk ^{4}He.[10] In this way we are able to estimate the chemical potential of one ^{6}He impurity in liquid ^{4}He and then the solubility of ^{6}He in ^{4}He.

B. Self-binding with glue SWF

In the present work we have also studied ^{6}He clusters. In order to describe the self-binding properties of quantum clusters we have extended our treatment of dishomogeneous ^{4}He systems with a free surface[12] to ^{6}He. Binding in a quantum system at $T=0$ K is peculiar because the dense system coexists with a vacuum, not a vapor as in a classical system. This means that the quantum probability density $P(R)=|\Psi_0(R)|^2$ cannot have a classical analogue with a system with local interparticle interactions. We noticed that the following form of Ψ_0 has the desired properties:

$$\Psi_G(R)=\int dS\ \ F(R,S)\times L(S). \tag{3}$$

The glue factor $L(S)$ has the form

$$L(S)=\prod_{i=1}^{N}\exp\left[-D\frac{(\hat{n}_i-1)^2}{\hat{n}_i}\right]. \tag{4}$$

$\hat{n}_i$ represents a suitably normalized local-density operator of shadow variables around the ith shadow and we have used the form

TABLE I. Variational parameters optimized for the SWF (1) at some densities for bulk ^{6}He, together with the variational energy per particle. Lengths are in units of $\sigma=2.556$ Å.

ρ Å^3	b/σ	$C\sigma^2$	$\alpha\sigma$	δ	$\langle E\rangle/N$[K]	State
0.02186	1.1	7.2	0.915	0.11	−11.55(3)	L
0.02620	1.11	7.8	0.91	0.11	−12.86(2)	L
0.02844	1.11	7.8	0.91	0.13	−13.18(2)	L
0.0294	1.11	7.8	0.91	0.13	−13.24(3)	L
0.03161	1.11	7.8	0.91	0.13	−14.39(3)	S
0.03270	1.11	7.8	0.91	0.11	−14.50(3)	S
0.03485	1.11	8.3	0.91	0.11	−14.39(2)	S
0.03703	1.11	8.5	0.91	0.11	−13.82(3)	S

$$\hat{n}_i=\frac{1}{A}\sum_{j(\neq i)} l(|\vec{s}_i-\vec{s}_j|),\ \ l(s)=e^{-\mu s^2}. \tag{5}$$

The correlations introduced by the glue factor $L(S)$ act as a ''spring,'' trying to keep $\hat{n}_i$ not too far from 1. When the system is homogeneous the argument for the exponential function in $L(S)$ can be expanded around the average value $\langle\hat{n}_i\rangle$, and to the lowest order in $\hat{n}_i-\langle\hat{n}_i\rangle$ the effect of the glue factor $L(S)$ is simply a renormalization of the Jastrow factor f_s for shadow. To second order, it introduces triplet correlations between shadow variables. The situation is completely different if the homogeneous state is such that $\langle\hat{n}_i\rangle$ is much below unity. This is the case in which N atoms have a very large volume V available so that the average density is much below the equilibrium density of the system. In this case the glue term causes a symmetry breaking in the state of the system, i.e., the N atoms do not fill uniformly the volume V but only partially in order to let the value of $\hat{n}_i$ be close to unity in that portion of V that is occupied by particles. The remaining region has zero density. In fact the probability that a single particle can escape from the fluid is zero due to the presence of $\hat{n}_i$ in the denominator in the exponential of Eq. 4: a configuration in which one ^{6}He atom that is far from the rest of the system causes $\hat{n}_i$ to be near zero and therefore also $L(S)$ so that the SWF vanishes for such configurations. In principle we could have evaporation of dimers or trimers but the actual computation shows that this never happens when the wave function is optimized. In this way we are able to reproduce the self-bound properties of ^{6}He in the presence of a free surface. Among the new variational parameters contained in $L(S)$, D controls the force of the ''spring,'' μ characterizes the range of the local-density operator, and A controls the average density of the system.

III. RESULTS

A. Bulk ^{6}He

We have studied bulk ^{6}He at different fixed densities in a simulation box with $N=108$ particles with periodic boundary conditions. Typical runs generate 5×10^5 Monte Carlo steps after 5×10^4 steps used to equilibrate the starting configuration. In Table I we report the variational parameters

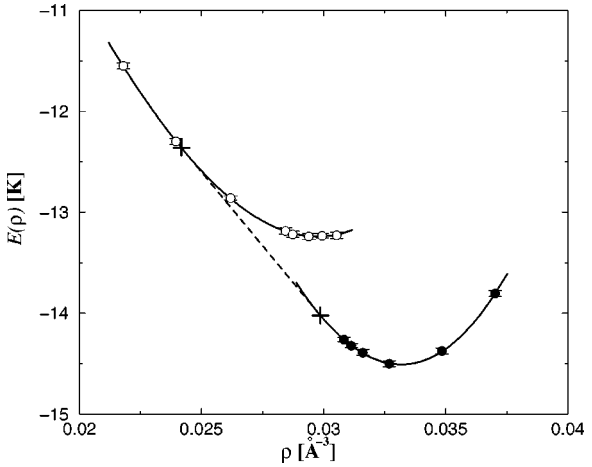

FIG. 1. Equation of state of ^{6}He at $T=0$. The lowest branch represents the solid phase. Crosses represent freezing and melting densities in the metastable region at negative pressure.

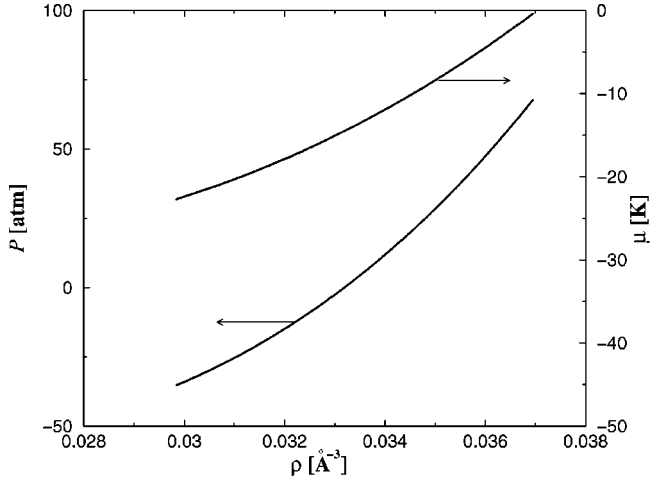

FIG. 2. Pressure P and chemical potential μ for bulk solid ^{6}He at $T=0$.

optimized for the bulk ^{6}He system at some densities together with the variational energy per particle. The simulation box for the solid phase has been kept cubic in order to stabilize the fcc lattice. The full equation of state is shown in Fig. 1. The lines are fits to the calculated energies per particle with a cubic polynomial of the form

$$E(\rho)=E_0+B[(\rho-\rho_0)/\rho_0]^2+C[(\rho-\rho_0)/\rho_0]^3. \quad (6)$$

The parameters of the fit are reported in Table II. From the fitted equation of state we can calculate the equilibrium $\rho_{eq}=0.033\,19$, freezing $\rho_{fr}=0.029\,84$, and melting densities $\rho_{mel}=0.024\,17$ Å^{-3}. We confirm that on the basis of our microscopic theory, the ground state of ^{6}He at $T=0$ is solid but the energy difference between the two phases is rather small. From the equation of state it is possible to obtain a number of different physical quantities of the system such as the pressure and chemical potential; these are shown in Fig. 2 for the solid phase.

B. One ^{6}He impurity in ^{4}He

We have also studied ground- and excited-state properties of a system composed of one ^{6}He impurity in liquid ^{4}He. In this system the interatomic interaction between the ^{6}He impurity and ^{4}He atoms is equal to the one between ^{4}He; therefore, the ^{6}He atom differs from the ^{4}He atoms only for its bare mass. As already done in the case of one ^{3}He impurity,[10] the correlating factors in the SWF for ^{6}He-^{4}He and ^{4}He-^{4}He are assumed for simplicity to be equal. The chemical potential of the ^{6}He impurity at the equilibrium density of ^{4}He turns out to be $\mu_6^{imp}=-10.0\pm0.6$ K. This result gives us the possibility to obtain the solubility x of ^{6}He in ^{4}He at low temperatures. The equilibrium condition for a solution of ^{6}He in ^{4}He is given by the following relation between the chemical potential of pure ^{6}He μ_6, the impurity chemical potential μ_6^{imp}, and the solubility x of ^{6}He in ^{4}He:

$$\mu_6=\mu_6^{imp}+k_BT\ln x. \quad (7)$$

From the value of $\mu_6=E_0$ at the equilibrium density $\rho=0.03319$ Å^{-3} and from the value of μ_6^{imp} we obtain the solubility of ^{6}He in ^{4}He: $x\simeq\exp(-4.43\ \mathrm{K}/T)$.

We have also studied excited-state properties of one ^{6}He impurity in liquid ^{4}He. We write the shadow wave function for an excited ^{6}He atom in the form

$$\Psi_q^I(R)=\int dS F(R,S)\,\delta_q^-, \quad (8)$$

where the momentum carrying factor reads

$$\delta_q^-=e^{i\vec{q}\cdot\vec{s}_{imp}}, \quad (9)$$

where $R=\{\vec{r}_{imp},\vec{r}_1,\ldots,\vec{r}_N\}$ are the coordinates of the particles (the subscript *imp* refers to the ^{6}He impurity variables; the others refer to ^{4}He atoms) and similarly for the shadows $S=\{\vec{s}_{imp},\vec{s}_1,\ldots,\vec{s}_N\}$. In this simulation we have computed directly the excitation spectrum of the ^{6}He impurity without performing the orthogonalization with the collective mode as done recently with the ^{3}He impurity case.[10] This is not a crude approximation because in that calculation we have found that the orthogonalization-diagonalization process has strong influence only on the spectrum of the collective excitations. It should be kept in mind that the present calculation of the excitation spectrum of the ^{6}He impurity is not as accurate as in the case of the ^{3}He impurity because we have not used an explicit backflow term in the expression of the excited state in order to optimize its contribution. It is known[11] in fact that introducing the phase in the subsidiary

TABLE II. Parameters of the fitted equation of state.

	Liquid	Solid
E_0	−13.240	−14.507
B	28.193	50.411
C	17.369	17.308
ρ_0	0.0298	0.0332

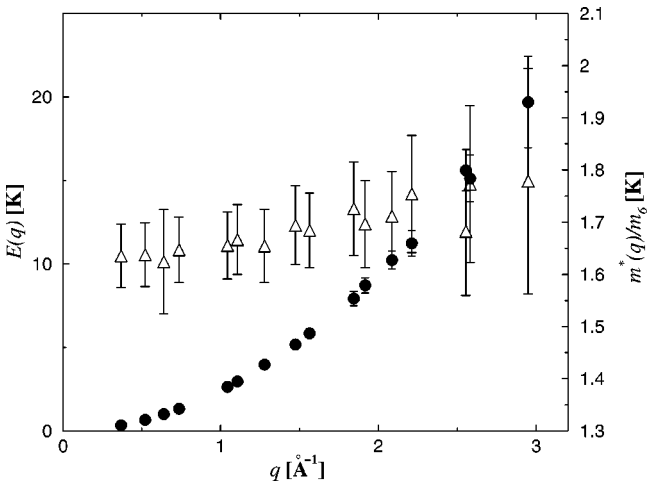

FIG. 3. Filled circles: excitation spectrum of a ^{6}He impurity in liquid ^{4}He at equilibrium density; triangles: effective mass of the ^{6}He impurity in m_6 units.

variables is a way to implicitly incorporate backflow up to high order in the real variables. However this contribution is determined by the ground-state pseudopotentials and in general it is not optimized. Backflow can be optimized only by introducing an explicit backflow term, which we have not done in the present computation. For this reason the present estimation of the effective mass of the ^{6}He impurity in liquid ^{4}He should be considered only as a lower bound. The excitation spectrum of the ^{6}He impurity is shown in Fig. 3 together with the wave-vector dependence of the effective mass of the ^{6}He impurity. Our computation can be performed only for a discrete set of q values such that the periodic boundary conditions of the simulation box are satisfied. Our theoretical quasiparticle excitation spectrum shows little deviation from a simple parabola. The values of the effective mass for the ^{6}He impurity range from $1.6–1.75m_6$ between $q=0.37$ and 3 Å^{-1}, where m_6 is the ^{6}He atomic mass. The deviation of the quasiparticle spectrum from the parabolic behavior is smaller than the one found in the ^{3}He impurity case. Moreover the renormalization of the mass of the ^{6}He impurity turns out to be less than that of the ^{3}He impurity;[10] this is probably due to the absence, in the present case, of an explicit backflow term in the wave-function. This term in fact has been able to increment the variational estimation of the ^{3}He impurity effective mass from $1.74–2.05m_3$ when used in SWF.

C. ^{6}He clusters

In the variational optimization of the wave function (3) we have performed an optimization of all its variational parameters and not only of those contained in the glue factor (4), as done in previous simulations of ^{4}He clusters. This has been necessary because we have seen evidence that as the dimension of the ^{6}He clusters increases, one goes from a high-density liquid to a system that tends to become a solid in the bulk limit. The sign that there is a substantial modification of correlations in these systems as their size increases can be seen in how we have to modify the variational parameters contained in $F(R,S)$ in order to optimize the wave function. In Table III we report the variational parameters optimized for ^{6}He clusters with different numbers of particles together with the variational energy per particle. In Figs. 4 and 5 we show the density profiles for three ^{6}He clusters with different numbers of particles; in particular in Fig. 4 the origin of the density profiles coincides with the center of the mass of the clusters, whereas in Fig. 5 the origin of the density profiles coincides with the ^{6}He atom nearest the center of the mass of the cluster; in this way it is possible to also analyze the amplitude of the density oscillations around an ^{6}He atom inside the cluster. In all the density profiles one can see the presence of a shell structure; moreover the oscillations in the density profiles centered in the ^{6}He atom nearest the center of the mass of the cluster become so high in density that it is possible that the inner part of these clusters becomes solid. In order to investigate this, we have analyzed the local order of ^{6}He atoms around the one nearest the center of the mass of the cluster, studying four-body angular correlations in the same way as we did[8] to

TABLE III. Variational parameters optimized for ^{6}He clusters with different numbers of particles N, simulated via the SWF (3). Lengths are in units of $\sigma=2.556$ Å.

N	b/σ	$C\sigma^2$	$\alpha\sigma$	δ	D	$\mu\sigma^2$	A	$\langle E\rangle/N$[K]
20	1.11	7.8	0.98	0.09	0.45	0.1	45	−3.86(2)
40	1.12	7.8	0.98	0.09	0.45	0.1	55	−5.22(1)
65	1.12	7.8	0.98	0.09	0.45	0.1	70	−5.16(1)
70	1.12	7.8	0.98	0.09	0.45	0.1	75	−6.29(1)
112	1.11	7.6	0.92	0.11	0.45	0.1	85	−7.11(1)
125	1.11	7.6	0.92	0.11	0.45	0.1	88	−7.32(1)
217	1.11	7.5	0.92	0.11	0.45	0.1	100	−8.22(1)
240	1.11	7.5	0.92	0.11	0.45	0.1	105	−8.37(1)
500	1.11	7.2	0.92	0.11	0.45	0.1	110	−9.35(1)
1000	1.11	7.2	0.91	0.11	0.45	0.1	130	−10.10(2)

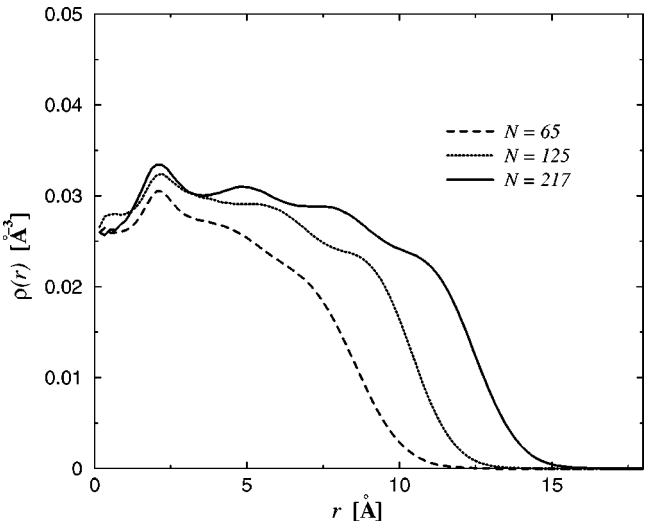

FIG. 4. Radial density profiles $\rho(r)$ for three ^{6}He clusters with different numbers of particles N. The origin coincides with the center of the mass of the clusters.

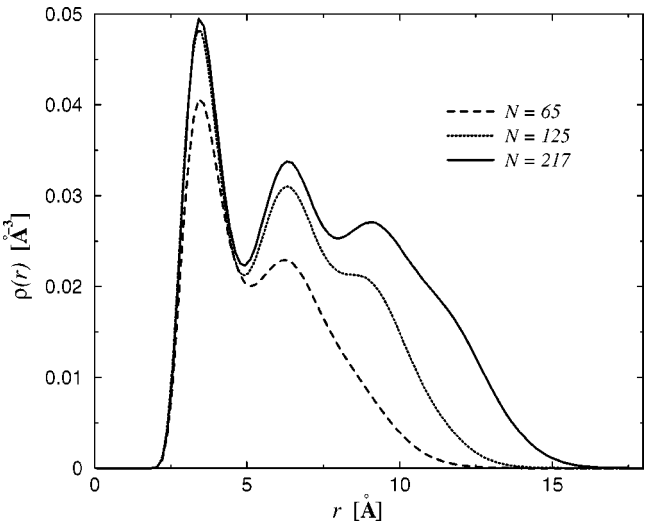

FIG. 5. Radial density profiles $\rho(r)$ for three ^{6}He clusters with different numbers of particles N. In this case the origin is fixed to the coordinate of the ^{6}He atom nearest the center of the mass of the cluster.

analyze the local solid order around the SF_6 molecule or the K^+ ion in ^{4}He systems. This analysis consists of choosing two of the ^{6}He atoms in the first shell around the ^{6}He atom nearest the center of the mass of the cluster (which is taken as the origin of coordinates). One of these two atoms is used to fix the z axis, and the second is used to define the x-y plane. Having oriented the coordinate axis in this way we analyze the statistics $P(\theta,\phi)$ for the angles at which the other ^{6}He atoms are found. The result for an ^{6}He cluster with $N=217$ atoms is shown in Fig. 6. One can see that only

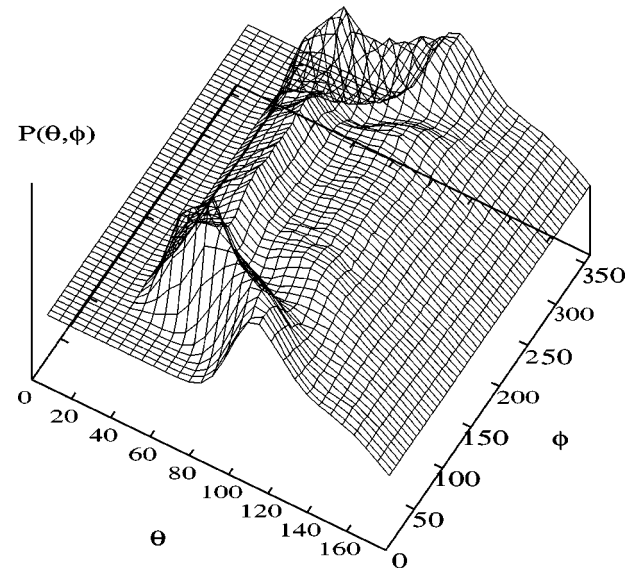

FIG. 6. Probabilty function $P(\theta,\phi)$ to find a ^{6}He at angles (θ,ϕ) having one fixed ^{6}He on the z axis and one on the x-y plane (in this case $\theta \simeq 60°$). The cluster has $N=217$ ^{6}He atoms. The origin of the coordinates is the ^{6}He atom nearest the center of the mass of the cluster, and this analysis is performed only with the ^{6}He belonging to the first shell ($2<r<5$ Å) around this atom.

short-range order is present with no definite sign of solidlike order. It should be noticed that these angular correlations become more and more pronounced as the size of the clusters increases. It is instructive to consider the case of a cluster of ^{4}He with one impurity ion such as K^+. In this case we find[13] a highly ordered first shell of ^{4}He atoms around the ion as shown by the presence of well-defined peaks in $P(\theta,\phi)$ extending over all directions (θ,ϕ). In addition the radial density profile shows more pronounced oscillations than in the present case of ^{6}He. We conclude that a cluster of a few hundered ^{6}He atoms is in a state intermediate between a liquid and a solid in which there is a pronounced layering but no well-defined angular correlations. Presumably one needs a substantially larger cluster in order for a well-defined solid order to become stabilized.

IV. BOSE-EINSTEIN CONDENSATION AND MOMENTUM DISTRIBUTION

The disordered state of a cluster of ^{6}He atoms suggests that it is superfluid at low-enough temperature. With our technique we are not able to assess superfluidity but we can study the presence of Bose-Einstein condensation in our small liquid ^{6}He clusters. In a strongly interacting system like the present one, the property of off-diagonal long-range order (ODLRO) in the one-body density matrix[14] characterizes the presence of Bose-Einstein condensation. The one-body density matrix is defined by

$$\rho_1(\vec{r},\vec{r}') = N \int d\vec{r}_2 \ldots d\vec{r}_N \Psi(\vec{r},\vec{r}_2,\ldots,\vec{r}_N) \times \Psi(\vec{r}',\vec{r}_2,\ldots,\vec{r}_N); \quad (10)$$

this function is related to the momentum distribution simply by a Fourier transform, so in the bulk system the presence of ODLRO in $\rho_1(\vec{r},\vec{r}')$ ($\lim_{|\vec{r}-\vec{r}'|\to\infty}\rho_1 \neq 0$) implies a macro-

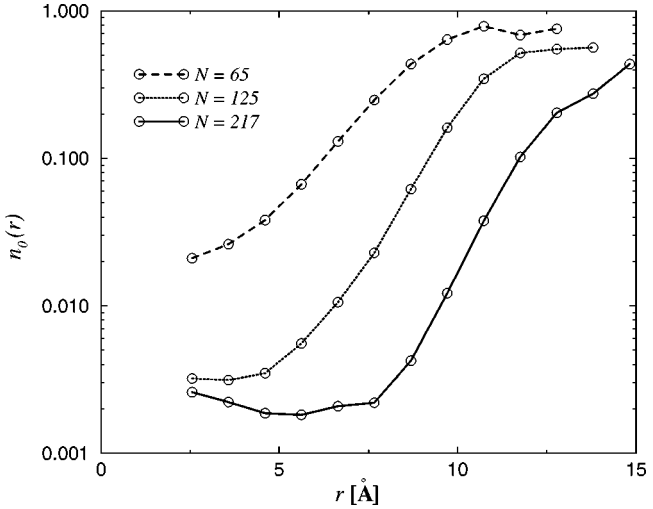

FIG. 7. Estimation of the local condensate fraction $n_0(r)$ for three ^{6}He clusters with different numbers of particles N. For $r<2.5$ Å, $n_0(r)$ is not shown because the long-range limit is not reached. Notice the logarithmic scale for n_0.

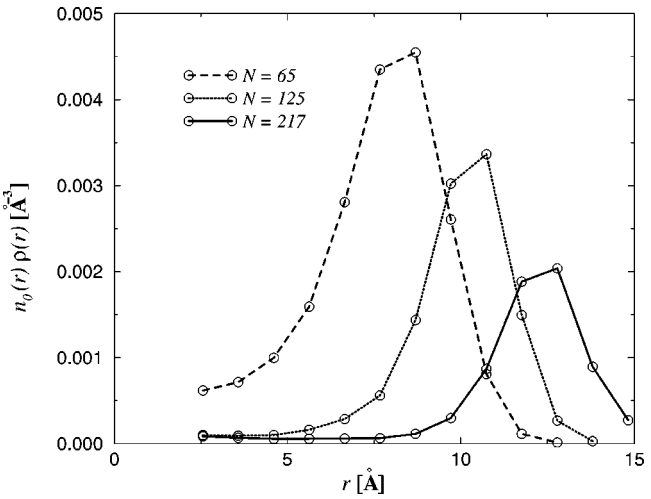

FIG. 8. $n_0(r)\times\rho(r)$ for the three ^{6}He clusters of the previous figure.

scopic occupation of the zero-momentum state, i.e., Bose-Einstein condensation. A cluster is a finite system, so it is not possible to extend to infinity the off-diagonal limit of the one-body density matrix and a genuine Bose-Einstein condensate cannot exists.[15] However, it is possible to study the off-diagonal behavior of $\rho_1(\vec{r},\vec{r}')$, increasing the number of atoms in the cluster in order to extrapolate the results to an infinite system. In the spherical geometry of a cluster the one-body density matrix is a function of the modulus of $\vec{r}$ and $\vec{r}'$ and the angle ϕ between $\vec{r}$ and $\vec{r}'$ $\rho_1(\vec{r},\vec{r}')=\rho_1(r,r',\phi)$. As shown by Krotscheck,[16] in an inhomogeneous system when $\vec{r}$ and $\vec{r}'$ are far apart, the one-body density matrix approaches a nonzero limit

$$\rho_1(r,r',\phi)\simeq[\rho(r)\rho(r')n_0(r)n_0(r')]^{1/2} \qquad (11)$$

and this allows us to define the local condensate fraction at distance r from the center of the mass of the cluster; $\rho(r)$ is the density profile of the cluster. We have studied the one-body density matrix $\rho_1(\vec{r},\vec{r}')$ in ^{6}He clusters with $\vec{r}$ and $\vec{r}'$ that lie on circumferences with the center in the center of the mass of these clusters; that is $r=r'$. In this way the off-diagonal long-range limit is reached when the angle ϕ between $\vec{r}$ and $\vec{r}'$ is about π: in a cluster with a diameter larger than the healing length we have approximately

$$n_0(r)=\rho_1(r,r,\phi\simeq\pi)/\rho(r). \qquad (12)$$

In Fig. 7 we show the local condensate fraction $n_0(r)$ computed in this way for three ^{6}He clusters with different numbers of particles ($N=65$, 125, 217). In Fig. 8 we show instead the product $n_0(r)\times\rho(r)$ between the local condensate fraction and the radial density of the same three ^{6}He clusters. Our results show that there is always a sizeable condensate in these clusters. In the inner part of the cluster the value of $n_0(r)$ strongly decreases as the size of the cluster increases and this reflects the building up of a more ordered structure. The value of $n_0(r)$ in all cases is about 10% in the region of the last shell of atoms in the cluster and $n_0(r)$ becomes even larger as we move in the tail of the density profile. This last behavior is similar to what is found in clusters of ^{4}He atoms. However as in the case of ^{4}He, the local condensate never reaches its maximum value of unity (100% condensation) even at the lowest densities in the tail of the density profile and this has been interpreted as an effect of the zero-point motion of surface fluctuations. In summary we find that in the surface region of a ^{6}He cluster there is always a rather large condensate whereas in the central region the value of n_0 strongly decreases in large clusters. In order to investigate the strength of this effect we have computed the total number N_c of condensed ^{6}He atoms in each cluster. These values turn out to be $N_c=15.3$ when $N=65$, $N_c=14.7$ when $N=125$, and $N_c=13.0$ when $N=217$. These results indicate that as their size increases, the core region of these clusters is going towards a phase transition from a liquid to a solid where BEC is not present or it has a very small value.

V. CONCLUSIONS

We find that the ground state of bulk ^{6}He is solid, in agreement with earlier results. However finite-size effects as found in clusters have a strong disordering effect on the system. In fact we find that even clusters of a few hundred atoms do not show a well-defined solid order. At the same time we find that there is a significant off-diagonal long-range order so that Bose-Einstein condensation is present in such clusters and superfluidity should be present. Therefore clusters of ^{6}He offer the unique opportunity to study the evolution from a superfluid to a solid and this is driven by size effect. Due to the marginal stability of the solid phase it is quite possible that even the solid, like clusters, have a finite Bose-Einstein condensate and the solid might have supersolid properties. Unfortunately our theory is limitated to $T=0$ K and we cannot compute the superfluid fraction. A path-integral Monte Carlo computation should be able to assess these questions. The prospect of producing ^{6}He clusters in free space is rather dim but it should be possible to produce such clusters inside bulk ^{4}He as a result of phase separation. We do not expect that inclusion of a few hundred atoms of ^{6}He in liquid ^{4}He will produce properties very different from those of clusters of ^{6}He atoms in free space.

ACKNOWLEDGMENTS

We thank G. L. Masserini for carrying out some preliminary calculations in this work. This work was supported by the INFM Parallel Computing Initiative.

[1] C. Raman, M. Kohl, R. Onofrio, D.S. Durfee, C.E. Kuklewicz, Z. Hadzibabic, and W. Ketterle, Phys. Rev. Lett. **83**, 2502 (1999).
[2] P. Sindzingre, D.M. Ceperley, and M.L. Klein, Phys. Rev. Lett. **67**, 1871 (1991).
[3] L. Guttman and J.R. Arnold, Phys. Rev. **92**, 547 (1953).
[4] L.H. Nosanow, J. Low Temp. Phys. **23**, 605 (1976).
[5] L.H. Nosanow, L.J. Parish, and F.J. Pinski, Phys. Rev. B **11**, 191 (1975).
[6] S. Moroni, D.E. Galli, S. Fantoni, and L. Reatto, Phys. Rev. B **58**, 909 (1998).
[7] F. Pederiva, A. Ferrante, S. Fantoni, and L. Reatto, Phys. Rev. Lett. **72**, 2589 (1994).
[8] C.C. Duminuco, D.E. Galli, and L. Reatto, Physica B **284-288**, 109 (2000).
[9] R.A. Aziz, V.P.S. Nain, J.S. Carley, W.L. Taylor, and G.T. McConville, J. Chem. Phys. **70**, 4330 (1979).
[10] D.E. Galli, G.L. Masserini, and L. Reatto, Phys. Rev. B **60**, 3476 (1999).
[11] L. Reatto, S.A. Vitiello, and G.L. Masserini, J. Low Temp. Phys. **93**, 879 (1993).
[12] D.E. Galli and L. Reatto, J. Phys.: Condens. Matter **28**, 6009 (2000).
[13] M. Buzzacchi, D.E. Galli, and L. Reatto (unpublished).
[14] O. Penrose and L. Onsager, Phys. Rev. **104**, 576 (1956).
[15] C.E. Campbell, J. Low Temp. Phys. **93**, 907 (1993).
[16] E. Krotscheck, Phys. Rev. B **32**, 5713 (1985).